8-16-2004

Carbonyl sulfide and carbon disulfide: Large-scale distributions over the western Pacific and emissions from Asia during TRACE-P

Nicola J. Blake
University of Colorado, Boulder

David G. Streets
Argonne National Laboratory

Jung -Hun Woo
University of Iowa

Isobel J. Simpson
University of California, Irvine

Jonathan Green
University of California, Irvine

See next page for additional authors

Recommended Citation

Blake, N. J., et al. (2004), Carbonyl sulfide and carbon disulfide: Large-scale distributions over the western Pacific and emissions from Asia during TRACE-P, J. Geophys. Res., 109, D15S05, doi:10.1029/2003JD004259.

Authors

Nicola J. Blake, David G. Streets, Jung -Hun Woo, Isobel J. Simpson, Jonathan Green, Simone Meinardi, Kazuyuki Kita, E L. Atlas, H Fuelberg, Glen Sachse, Melody A. Avery, S Vay, R. Talbot, Jack E. Dibb, A R. Bandy, D C. Thornton, F Sherwood Rowland, and D R. Blake

Carbonyl sulfide and carbon disulfide: Large-scale distributions over the western Pacific and emissions from Asia during TRACE-P

Nicola J. Blake,[1] David G. Streets,[2] Jung-Hun Woo,[3] Isobel J. Simpson,[1] Jonathan Green,[1,4] Simone Meinardi,[1] Kazuyuki Kita,[5] Elliot Atlas,[6] Henry E. Fuelberg,[7] Glen Sachse,[8] Melody A. Avery,[8] Stephanie A. Vay,[8] Robert W. Talbot,[9] Jack E. Dibb,[9] Alan R. Bandy,[10] Donald C. Thornton,[10] F. Sherwood Rowland,[1] and Donald R. Blake[1]

[1] An extensive set of carbonyl sulfide (OCS) and carbon disulfide (CS_2) observations were made as part of the NASA Transport and Chemical Evolution over the Pacific (TRACE-P) project, which took place in the early spring 2001. TRACE-P sampling focused on the western Pacific region but in total included the geographic region 110°E to 290°E longitude, 5°N to 50°N latitude, and 0–12 km altitude. Substantial OCS and CS_2 enhancements were observed for a great many air masses of Chinese and Japanese origin during TRACE-P. Over the western Pacific, mean mixing ratios of long-lived OCS and shorter-lived CS_2 showed a gradual decrease by about 10% and a factor of 5–10, respectively, from the surface to 8–10 km altitude, presumably because land-based sources dominated their distribution during February through April 2001. The highest mean OCS and CS_2 levels (580 and 20 pptv, respectively, based on 2.5° × 2.5° latitude bins) were observed below 2 km near the coast of Asia, at latitudes between 25°N and 35°N, where urban Asian outflow was strongest. Ratios of OCS versus CO for continental SE Asia were much lower compared to Chinese and Japanese signatures and were strongly associated with biomass burning/biofuel emissions. We present a new inventory of anthropogenic Asian emissions (including biomass burning) for OCS and CS_2 and compare it to emission estimates based on regional relationships of OCS and CS_2 to CO and CO_2. The OCS and CS_2 results for the two methods compare well for continental SE Asia and Japan plus Korea and also for Chinese CS_2 emissions. However, it appears that the inventory underestimates Chinese emissions of OCS by about 30–100%. This difference may be related to the fact that we did not include natural sources such as wetland emissions in our inventory, although the contributions from such sources are believed to be at a seasonal low during the study period. Uncertainties in OCS emissions from Chinese coal burning, which are poorly characterized, likely contribute to the discrepancy. *INDEX TERMS:* 0322 Atmospheric Composition and Structure: Constituent sources and sinks; 0345 Atmospheric Composition and Structure: Pollution—urban and regional (0305); 0365 Atmospheric Composition and Structure: Troposphere—composition and chemistry; 0368 Atmospheric Composition and Structure: Troposphere—constituent transport and chemistry; *KEYWORDS:* carbonyl sulfide (OCS), carbon disulfide (CS_2), Asian emissions, emission inventories

[1]Department of Chemistry, University of California, Irvine, California, USA.

[2]Argonne National Laboratory, Argonne, Illinois, USA.

[3]Center for Global and Regional Environmental Research, Iowa Advanced Technology Labs, University of Iowa, Iowa City, Iowa, USA.

[4]Now at Division of Chemistry and Chemical Engineering, California Institute of Technology, Pasadena, California, USA.

[5]Department of Environmental Sciences, Faculty of Science, Ibaraki University, Mito, Japan.

[6]National Center for Atmospheric Research, Boulder, Colorado, USA.

[7]Department of Meteorology, Florida State University, Tallahassee, Florida, USA.

[8]NASA Langley Research Center, Hampton, Virginia, USA.

[9]Institute for the Study of Earth, Oceans, and Space, Climate Change Research Center, University of New Hampshire, Durham, New Hampshire, USA.

[10]Chemistry Department, Drexel University, Philadelphia, Pennsylvania, USA.

1. Introduction

[2] While SO$_2$ is the major form of anthropogenic sulfur released to the troposphere, the reduced sulfur components OCS and CS$_2$ also have appreciable anthropogenic sources. Both reduced gases are ultimately oxidized to SO$_2$ in the troposphere and/or stratosphere so may be relevant to global climate change. The high tropospheric abundance (~500 pptv) and long tropospheric lifetime (2–7 years [*Xu et al.*, 2002]) of carbonyl sulfide (OCS) make it the major nonvolcanic source of sulfur to the upper atmosphere. *Crutzen* [1976] hypothesized that atmospheric OCS is the primary source of the stratospheric sulfate aerosol layer, which is highly effective in reflecting incoming solar radiation back to space, enhancing the global albedo [*Charlson et al.*, 1990].

[3] OCS is released to the atmosphere by oceans, biomass burning, the oxidation of carbon disulfide (CS$_2$) and dimethyl sulfide (DMS), and several anthropogenic sources (including aluminum production, coal combustion, and sulfur recovery). It is removed by terrestrial vegetation, soils, photolysis, and reactions with OH and O radicals [*Khalil and Rasmussen*, 1984; *Chin and Davis*, 1993; *Andreae and Crutzen*, 1997; *Watts*, 2000]. Terrestrial vegetation is recognized as a significant sink of atmospheric OCS, but the magnitude of this sink has not been satisfactorily quantified [*Kettle et al.*, 2002a]. Ice core samples collected from Siple Dome, West Antarctica, suggest that human activities contribute approximately 25% of modern OCS to the atmosphere [*Aydin et al.*, 2002].

[4] The atmospheric budget of CS$_2$ is not well defined. Natural sources to the atmosphere include the rotting of organic material in the oceans, soil and marshes [*Khalil and Rasmussen*, 1984]. However, the variable atmospheric spatial distribution of CS$_2$ and high levels that have been measured in continental air masses, suggests that anthropogenic sources are dominant over oceans [e.g., *Bandy et al.*, 1993; *Watts*, 2000]. Major industrial sources include carbon black production, rayon manufacture, CS$_2$ production and use, and sulfur recovery (see section 3 for references). Once released, CS$_2$ is rapidly converted to OCS and SO$_2$ [*Chin and Davis*, 1993]

[5] The atmospheric implications of changing Asian emissions motivated NASA's Global Tropospheric Experiment (GTE) TRansport and Chemical Evolution over the Pacific (TRACE-P) project, which took place in the early spring 2001 and focused on industrial emissions from the Asian Pacific Rim. The primary scientific objective of TRACE-P was to determine the chemical composition of the Asian outflow over the western Pacific in order to understand and quantify the export of chemically and radiatively important trace gases and aerosols, and their precursors, from the Asian continent. Early spring was selected because it corresponds to a combination of continental convection and a strong westerly wind pattern, and thus a maximum of Asian outflow over the North Pacific [*Jacob et al.*, 2003].

[6] The focus of this manuscript is the anthropogenic emissions of OCS and CS$_2$ during TRACE-P. Measured values are compared to specially constructed anthropogenic emission inventories for these gases. There have been several previous attempts to estimate global emissions of OCS and CS$_2$ [*Turco et al.*, 1980; *Khalil and Rasmussen*, 1984; *Chin and Davis*, 1993; *Watts*, 2000]. Both anthropogenic and natural sources were examined in these studies with the aim of developing a global emissions budget. However, all these studies suffered from a lack of information on source types and measured emission factors for OCS and CS$_2$, as well as difficulties estimating the magnitude of the anthropogenic activity or extent of the natural source. Though relatively more information is available today on the sources of these species, large uncertainties still surround all estimates.

2. Experimental Method

[7] We collected whole air samples on board NASA DC-8 and P-3B aircraft during the TRACE-P project (late February to early April 2001), as reported by *Blake et al.* [2003]. The full geographic region of study ranged from 110°E to 290°E longitudes, and 5°N to 50°N latitudes, and included key flights off the coasts of China and Japan.

[8] Air was brought into the aircraft through an external air intake, and a stainless steel (grease free) bellows pump filled individual 2-L stainless steel canisters to about four atmospheres of pressure. Prior to deployment, the canisters were evacuated and subsequently filled with 20 torr of deionized, degassed water to improve the performance of the analytical system and the stability of certain compounds in the canisters [*Colman et al.* 2001]. Each canister is equipped with a stainless steel bellows valve to ensure sample integrity. The canisters were analyzed in the Blake-Rowland laboratory at the University of California, Irvine (UCI), typically within one week of sample collection. For analysis, sample air was preconcentrated at liquid nitrogen temperature (−196°C) on a stainless steel loop filled with glass beads. Immersing the sample loop in hot water revolatilized the 1520 cm^3 (STP) sample aliquot. The sample was then flushed to a splitter that partitioned it to five different streams, with each stream sent to one of five column-detector combinations. The nonmethane hydrocarbons and halocarbons that are referred to later were quantified using the combinations described by *Blake et al.* [2003]. The combination that was used to quantify the sulfur gases was a DB-5ms (J&W Scientific) column (60 m; i.d., 0.25 mm; film, 0.5 μm) coupled to an HP-5973 quadrupole Mass Spectrometric Detector. The mass spectrometer was placed in the single ion monitoring (SIM) mode, choosing the most abundant ion of each compound without interference. The ions selected for the sulfur compounds were OCS ion 60 m/z, CS$_2$ 76 m/z. Calibration was performed by comparison to a Scott Marrin standard containing 0.943 ± 0.047 ppmv OCS, and 0.933 ± 0.047 ppmv CS$_2$ diluted to the pptv range in UHP helium (which had been further purified by passing through a graphite/molecular sieve trap immersed in liquid nitrogen).

[9] To test the stability of these sulfur gases in our stainless steel canisters we performed canister integrity studies. Individual cans are filled with outside air and analyzed immediately, then reanalyzed several more times over the following week or so. These tests have shown that OCS and CS$_2$ are stable (i.e., statistically there was no

difference between the first and last samples) in our canisters for storage times of more than one week.

[10] The measurement precision for OCS and CS$_2$ was 5%. The detection limit for CS$_2$ was 0.5 pptv, while that for OCS was better than 20 pptv. OCS was always present above its detection limit.

[11] High precision measurements of carbon dioxide (CO$_2$) were made on both the P-3B and DC-8 by modified Li-COR model 6252 nondispersive infrared (NDIR) spectrometers to an accuracy and precision of 0.25 and 0.07 ppmv, respectively [Vay et al., 1999]. High-precision measurements of carbon monoxide (CO) aboard the aircraft were made by fast response tunable diode laser sensors: the DACOM (Diferential Absorption CO Measurement) instrument on the DC-8 and the DACOM II instrument on the P-3b with a precision of 1% or 1 ppbv [Sachse et al., 1987].

[12] As the sampling frequencies of the in situ CO and CO$_2$ instruments are much higher than our whole air sampling, we have employed a merged data file generated at Harvard University containing CO and CO$_2$ mixing ratios averaged over the whole air sampling times. The TRACE-P measurements and merged data files are archived at the NASA Langley Research Center and can be accessed from http://www-gte.larc.nasa.gov/.

3. Anthropogenic Emissions Inventory for OCS and CS$_2$

[13] This paper estimates anthropogenic emissions of OCS and CS$_2$ in Asia, to aid in the interpretation of observations taken during the TRACE-P mission. We take advantage of year 2000 activity levels already compiled for Asia to support emission estimates of other species for TRACE-P [Streets et al., 2003]. Natural sources and the oxidation of CS$_2$ to OCS are not included in this inventory for reasons that are discussed later.

[14] Emission factors for anthropogenic sources of OCS and CS$_2$ are few and developed from extremely limited measurements. This adds greatly to the uncertainty of the emission estimates. Surprisingly, there are very few reported emission factors for combustion. Only one reported measurement of OCS emissions from coal combustion was found, with a measured OCS/CO$_2$ ratio of $2.3 \times 10^{-6} (=4.9 \times 10^{-3}$ g OCS kg^{-1} coal burned) at the Cherokee Power Plant in Denver, Colorado [Khalil and Rasmussen, 1984; Chin and Davis, 1993]. Whether this value holds for smaller coal combustors that are common in Asia is not clear; however, a similar value (5×10^{-3} g OCS kg^{-1} coal burned) is obtained if we convert the OCS mixing ratio of 60 ppbv measured in the chimney of a Beijing coal stove reported by Mu et al. [2002] to g OCS kg^{-1} coal burned. In the absence of further data we have used the measured U.S. power plant OCS/CO$_2$ ratio for all coal combustors. More information is available for CS$_2$: U.S. Environmental Protection Agency (USEPA) [2003] emission rate estimates for eight different types of coal combustor yield an emission factor of 6.5×10^{-5} g CS$_2$ kg^{-1} coal burned. Fried et al. [1992] measured OCS/CO mass ratios in automobile exhausts, yielding values of 5.8×10^{-6} for gasoline vehicles and 199×10^{-6} for diesel vehicles. These values were applied to the Asian population

of diesel and gasoline vehicles used in the emission inventory calculations of Streets et al. [2003]. In the absence of a literature estimate of the emission factor for the combustion of oil in boilers, we scaled transportation sector OCS emissions by the ratio of stationary-to-transport oil use in each region. No independent estimates of CS$_2$ emission rates from oil combustion were found, so emissions were estimated from OCS emissions, per Chin and Davis [1993]. A ratio of CS$_2$/OCS emissions from automobiles of 0.0825 was adopted for both mobile and stationary source oil combustion. For the combustion of biofuels in residential stoves and cookers we used a value of 0.04 g OCS kg^{-1} dry fuel burned [Andreae and Merlet, 2001]. Recommended values of Andreae and Merlet [2001] were also used for the open combustion of biomass, as follows: grassland, 0.015 g OCS kg^{-1} dry fuel burned; tropical forest, 0.04 g OCS kg^{-1} dry fuel burned; extratropical forest, 0.033 g OCS kg^{-1} dry fuel burned; and crop residue, 0.065 g OCS kg^{-1} dry fuel burned. There are no reports of CS$_2$ releases from the combustion of vegetation of any kind.

[15] Four major industrial processes were assessed for OCS emissions: carbon black production, aluminum production, pigment production, and sulfur recovery. Carbon black production data are taken from United Nations (UN) [1998], updated to 2000 using annual industrial growth factors by country. The emission factor is 10 g kg^{-1} of carbon black produced, according to USEPA [2003]. However, it is assumed that in Japan and Korea emissions are controlled with incinerators or similar technology, operating at 99% OCS removal. For aluminum production we use an emission factor of 4 g OCS kg^{-1} of aluminum produced [Harnisch et al., 1995] and annual production data from UN [1998]. For pigment production we assume that the emissions are associated with the production of TiO$_2$ for white pigment manufacture. Though we have been unable to locate an emission factor for this activity, we have estimated one based on reported information on OCS releases from the Millennium Chemical plant in Ashtabula, Ohio, according to its TRI filing [see http://www.greatlakesdirectory.org/oh/polluter0430.htm]: 14.7 g OCS kg^{-1} of TiO$_2$ produced. Production data are from UN [1998], as is information on amounts of sulfur recovered from a variety of industrial processes, which include coal-gas plants, refineries, natural gas processing plants, and lead and zinc sulfide ore processing plants. This list is more comprehensive than previous estimates. On the basis of analysis by Peyton et al. [1976], of the sulfur recovery systems in place in the United States in the early 1970s, we assume an emission rate of 0.263 g OCS kg^{-1} of sulfur recovered.

[16] For CS$_2$ emissions we assessed four major industrial sources: carbon black production, rayon manufacture, CS$_2$ production and use, and sulfur recovery. For carbon black production, we used the same activity data as for OCS and an emission factor of 30 g CS$_2$ kg^{-1} carbon black produced [USEPA, 2003]. Again, we assumed that emissions in Japan and Korea are controlled by incinerators or similar technology at 99% CS$_2$ removal. Rayon manufacture is the biggest user of CS$_2$ in industry. It has been reported that rayon manufacture consumes 65–80% of CS$_2$ produced [Chin and Davis, 1993]; we assume 75% in this study. Rayon production seems to be generally steady or decreasing in most of

the world, except for a slow increase in China [*UN*, 1998]. An emission rate of 251 g CS$_2$ kg^{-1} rayon produced was used [*USEPA*, 2003]. Emissions are assumed to be uncontrolled, except in Japan where a 16% annual reduction is assumed [*USEPA*, 2003]. The production of CS$_2$ and evaporative emissions from its use are also major sources of tropospheric CS$_2$. Production data for CS$_2$ [*UN*, 1998] are available for Japan; China data are from the *China National Chemical Information Centre* [2000]; estimates for other countries are prorated to rayon production. Following the work of *Chin and Davis* [1993], we assume that 7.5% of industrial CS$_2$ production is used as a solvent in miscellaneous industrial processes and that 80% (we assume 40% for Japan) of it is released into the atmosphere through evaporation. For sulfur recovery, we follow the same procedure as for OCS and assume an emission rate of 0.341 g CS$_2$ kg^{-1} sulfur recovered [*Peyton et al.*, 1976].

[17] There are two major sources of OCS and CS$_2$ from agricultural activities: rice paddies and animal feedlots. Rice paddy emissions were calculated using the same national areas of rice production as in the calculation of CH$_4$ emissions for the TRACE-P inventory [*Streets et al.*, 2003]. The emission factors used were 7.8 × 10^{-3} g OCS m^{-2} and 5.6 × 10^{-3} g CS$_2$ m^{-2}, cited by *Watts* [2000] based on measurements in tropical paddy fields by *Kanda et al.* [1992]. Similarly, numbers of different animals by country followed the TRACE-P CH$_4$ analysis [*Streets et al.*, 2003]. Amounts of manure generation were obtained from the *USEPA* [1992] in units of kg manure per head per day by type of animal. Emission factors of 0.00325 g OCS Mg^{-1} of manure produced and 0.00775 g CS$_2$ Mg^{-1} [*Banwart and Bremner*, 1975] were used for all animal types. Finally, releases from landfilled municipal waste were estimated from the amounts of waste landfilled in each region, again following the TRACE-P CH$_4$ calculations [*Streets et al.*, 2003]. The emission factors were estimated as the average of three air quality permits filed in the United States for operation of landfills (Cerbat Landfill, Kingman, Arizona; Cinder Lake Landfill, Flagstaff, Arizona; Oklahoma City Landfill, Oklahoma). The methodology used is from *USEPA* [2003, section 2.4.1]. The average emission rates were 0.116g OCS Mg^{-1} of waste landfilled and 0.178 g CS$_2$ Mg^{-1}. Uncertainties in our emission estimates are estimated as 95% confidence intervals, using the methodology described by *Streets et al.* [2003].

[18] Figure 1 presents the gridded emission distributions for OCS from anthropogenic and biomass burning sources, and for anthropogenic CS$_2$ emissions. We estimate that Asian anthropogenic emissions of OCS are 146 ± 75 Gg yr^{-1}. This is higher than might be expected from previous global inventories (see Table 1). We attribute this to higher emission factors for vegetation burning, of which biofuel combustion may or may not be included in these other inventories, and the inclusion of more industrial process types. The increased estimate for vegetation burning appears to be consistent with recent observations of enhanced OCS concentrations in the upper tropical troposphere attributed to biomass burning [*Notholt et al.*, 2003]. Overall, the major contributing anthropogenic OCS sources are biofuel combustion 39%, industrial production 24%, open biomass burning 21%, and rice paddies 7%. The largest contributing regions are China 37%, India 24%, and Southeast Asia 22%.

[19] We estimate that Asian anthropogenic emissions of CS$_2$ are 99 ± 65 Gg yr^{-1}. As first reported by *Chin and Davis* [1993], we find that the overwhelming contributor is industrial production (91%), arising mainly from the manufacture and use of CS$_2$ itself. Rice paddies contribute about 7%. The largest contributing regions are China 43%, India 30%, and Japan 18%.

4. Analysis of TRACE-P Data

4.1. Large-Scale Distributions

[20] The regional distributions of OCS and CS$_2$ measured in our whole air samples are illustrated as 2.5° × 2.5° latitude/longitude patches color-coded by the average mixing ratio in each patch (Figure 2). As expected for gases with continental sources, the highest mixing ratios generally are found at low altitudes close to the coasts of China and Japan. Mixing ratios of relatively short-lived CS$_2$ drop relatively rapidly with altitude and distance from the coast (Figure 2).

4.2. Vertical Distributions

[21] Over the western Pacific (<165°E), OCS and CS$_2$ mixing ratios were enhanced by at least 10% and by a factor of 5−10, respectively, in samples collected below 2 km altitude, compared to those collected at 8−10 km (Figure 3). Similarly strong gradients were observed for the anthropogenic tracer gas tetrachloroethene (C$_2$Cl$_4$) (Figure 3 and *Blake et al.* [2003]) and combustion marker ethyne (Figure 3), suggesting that boundary layer levels of OCS and CS$_2$ may have been strongly influenced by continental anthropogenic sources during TRACE-P. At low latitudes (<25°N) over the western Pacific, mean mixing ratios of both OCS and CS$_2$ were about 25 pptv (4.5%) and 12 pptv (50%) lower, respectively, compared to high latitudes (>25°N) (Figure 3). However, boundary layer levels of the oceanic tracer DMS (whose budget is dominated by oceanic emissions [e.g., *Watts*, 2000]) were also elevated close to the coast (Figure 3), suggesting that contributions from natural sources can not be ruled out.

[22] In contrast to DMS, mean levels of OCS and CS$_2$ (as well as C$_2$Cl$_4$) over the central and eastern Pacific at altitudes below about 4 km were significantly lower than those over the western Pacific (Figure 3). This is the result of a diminished influence from continental sources but also supports findings, recently summarized by *Watts* [2000], that in general, the fluxes of OCS and CS$_2$ from open ocean regions are much lower per unit area than from coastal areas. central and eastern Pacific OCS mixing ratios to the south of 25°N still exhibited a slight negative gradient with altitude (about 5%). However, in the northern region (>25°N) midtropospheric mixing ratios of OCS (between about 5 and 10 km) were higher than those observed at lower altitudes. They were also higher than those measured in the same latitude and altitude range but close to the Asian continent (Figure 3). Corresponding enhancements are also observed for the combustion/biomass burning tracer ethyne and CH$_3$Cl (Figure 3). These enhancements were principally the result of an extensive layer of biomass burning influenced air that was encountered to the NE of
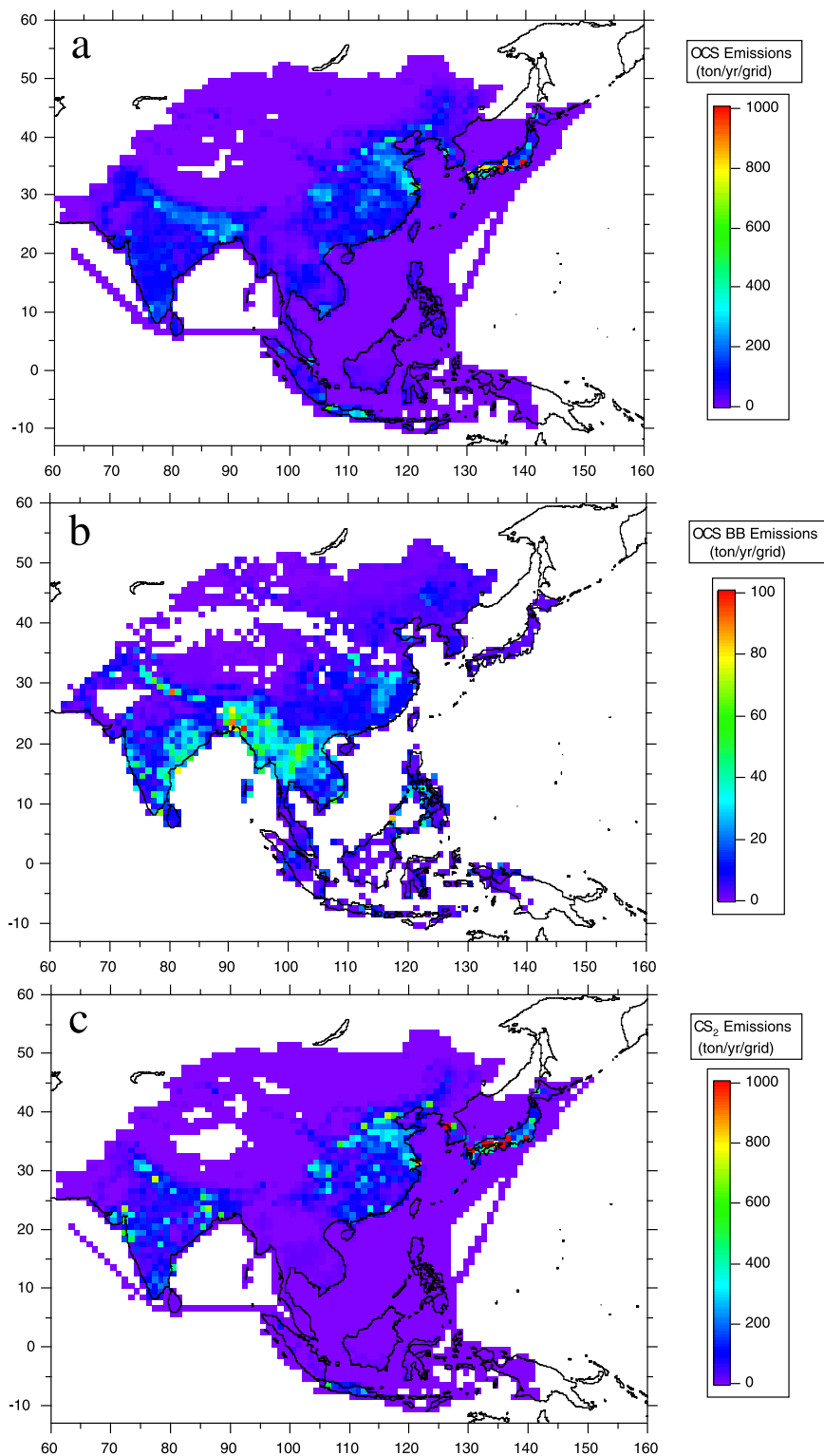
Figure 1. Maps of the gridded emission distributions of OCS from (a) anthropogenic sources, (b) biomass burning, and (c) anthropogenic CS$_2$ emissions. White areas represent very low emissions.

the Hawaiian Islands and was sampled in the course of several ascent/descents during the DC-8 transit flight 4 (Dryden, California, to Kona, Hawaii). OCS mixing ratios were 520–530 pptv, and enhanced mixing ratios of ethyne, CH$_3$Cl, and ozone (more than 80 ppbv O$_3$ [Blake et al., 2003]) were observed, but not the industrial tracer C$_2$Cl$_4$

(Figure 3). Backward trajectories reveal that the polluted air had originated at low altitude over Myanmar (Burma) and northern India approximately 5 days previously, regions that *Heald et al.* [2003] have characterized as the sites for many biomass fires throughout the TRACE-P period and identified as an OCS source region in Figure 1.

Table 1. Summary of Anthropogenic Emissions of OCS and CS$_2$ in Asia, With Global Estimates for Comparison[a]

Country/Region	Combustion					Industrial Production	Agriculture		Landfills	Total Anthropogenic	Total (Natural Plus Anthropogenic)
	Coal	Oil Plants	Biofuel	Transport	Biomass Burning		Rice Paddies	Animal Feedlots			
OCS											
China	4.4	1.4	19.9	1.4	8.5	15.7	2.3	0.006	0.009	53.7	
Japan	0.62	0.61	0.16	0.25	0.14	9.8	0.14	0.0002	0.002	11.7	
Rest of east Asia	0.62	0.24	0.87	0.16	0.89	0.26	0.15	0.0003	0.002	3.2	
Southeast Asia	0.27	0.48	13.0	0.52	12.6	2.4	3.3	0.002	0.003	32.5	
India	1.4	0.50	16.8	0.64	6.8	5.7	3.5	0.004	0.003	35.3	
Rest of south Asia	0.048	0.11	5.9	0.10	2.3	0.01	1.2	0.001	0.0005	9.7	
Asia total	7.3	3.4	56.6	3.1	31.2	33.9	10.7	0.01	0.02	146	
Global estimates											
Watts [2000]	36			6	70	82				194	1310
Khalil and Rasmussen [1984]	80			10	200	50				340	2000
Chin and Davis [1993]	36			4	140	2				182	1140
CS$_2$											
China	0.057	0.12	0	0.11	0	40.5	1.7	0.015	0.014	42.5	
Japan	0.007	0.051	0	0.020	0	17.3	0.099	0.0004	0.003	17.5	
Rest of east Asia	0.008	0.020	0	0.013	0	2.3	0.11	0.0009	0.003	2.5	
Southeast Asia	0.004	0.039	0	0.043	0	2.4	2.4	0.004	0.005	4.9	
India	0.021	0.041	0	0.053	0	26.8	2.5	0.010	0.004	29.4	
Rest of south Asia	0.0007	0.009	0	0.008	0	1.2	0.88	0.003	0.0009	2.1	
Asia total	0.097	0.28	0	0.25	0	90.5	7.7	0.03	0.03	99	
Global estimates											
Watts [2000]										340	660
Khalil and Rasmussen [1984]	0				0					370	2000
Chin and Davis [1993]	0			0.3	0	313				313	540

[a]Emissions are in Gg yr^{-1}.

Even though the plume was relatively fresh (ethene mixing ratios were present at nearly 70 pptv [*Blake et al.*, 2003]) concentrations of CS$_2$ were not significantly elevated above detection limit, consistent with biomass burning being a substantial source for OCS but not CS$_2$ (as stated in section 3). This pollution was also associated strongly with both fine and coarse aerosols, indicating that the fire emissions were lifted into the upper free troposphere by a process other than wet convection (possibly frontal lifting [*Liu et al.*, 2003]).

4.3. Latitudinal Distributions

[23] Mean OCS mixing ratios measured at low altitude (<2 km) over the western Pacific during TRACE-P were on average greater than those in the corresponding mid and upper troposphere between about 10°N and 35°N, with the negative vertical gradient maximizing between about 25°N and 35°N (Figure 4). CS$_2$ values were also most elevated at low altitudes between 25°N and 35°N, tapering off to the north and south of this latitude band. At midaltitudes (2–8 km) OCS levels gradually increased with latitude to produce an approximately neutral vertical gradient at about 40°N. The latitudinal/altitude distributions of both OCS and CS$_2$ were remarkably similar to gases with strong fossil fuel combustion sources, including CO, SO$_2$, and ethyne (Figure 4). Sulfur dioxide in particular is strongly associated with emissions from high sulfur Asian coal combustion [*Streets et al.*, 2003]. By comparison, Figure 1 suggests that the latitude band corresponding to the highest industrial emissions of OCS and CS$_2$ is slightly to the north, at 30°N to 40°N, which is consistent with prevailing offshore transport pathways during TRACE-P [*Fuelberg et al.*, 2003]. Ethane and propane have particularly strong latitudinal gradients which, in contrast to OCS and CS$_2$,

decrease very little at the highest northern latitudes (Figure 4). *Carmichael et al.* [2003] associate these high alkane levels with air mass flows from western Russia, where gas-processing activities in this region may be underestimated in the current emission inventories. However, the latitude distribution of DMS provides the greatest contrast to those of OCS and CS$_2$ (Figure 4). Natural ocean emissions, which dominate atmospheric DMS mixing ratios, appear to be stronger at southerly tropical latitudes close to the Asian coast.

5. Source Signatures

[24] The relative importance of various OCS sources probably varies widely between countries as well as between regions in large nations such as China, and therefore characteristic source trace gas signatures can vary widely, depending upon individual air mass trajectories. Anthropogenic C$_2$Cl$_4$ is a good general indicator of urban emissions, while CH$_3$Cl, the atmosphere's most abundant halocarbon, is emitted during biomass burning and has previously served as a useful biomass burning tracer [*Blake et al.*, 1996, 1999] but is also likely emitted as the result of biofuel use and coal burning.

5.1. Urban Plumes

[25] Table 2 presents the ratios of the changes (Δ) ΔOCS and ΔCS$_2$ to ΔCO and ΔCO$_2$ for selected plumes with 5-day air mass backward trajectories that exhibited interaction with specific urban areas that were sampled during DC-8 flights 8, 12, and 13. The backward trajectory calculations are described by *Fuelberg et al.* [2003]. The different plumes all have their own unique characteristics, but in general show elevated C$_2$Cl$_4$ and CH$_3$Cl, as well as
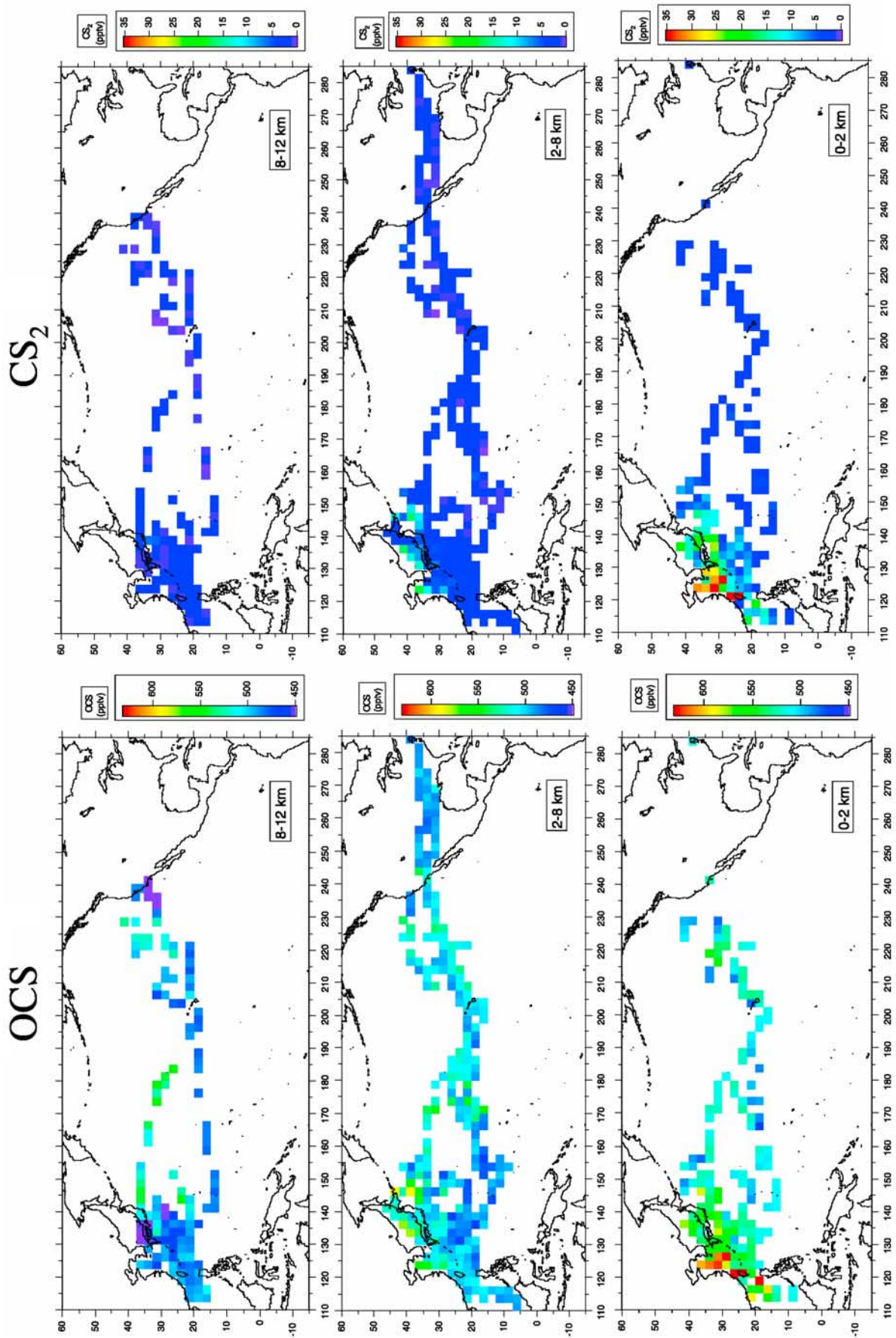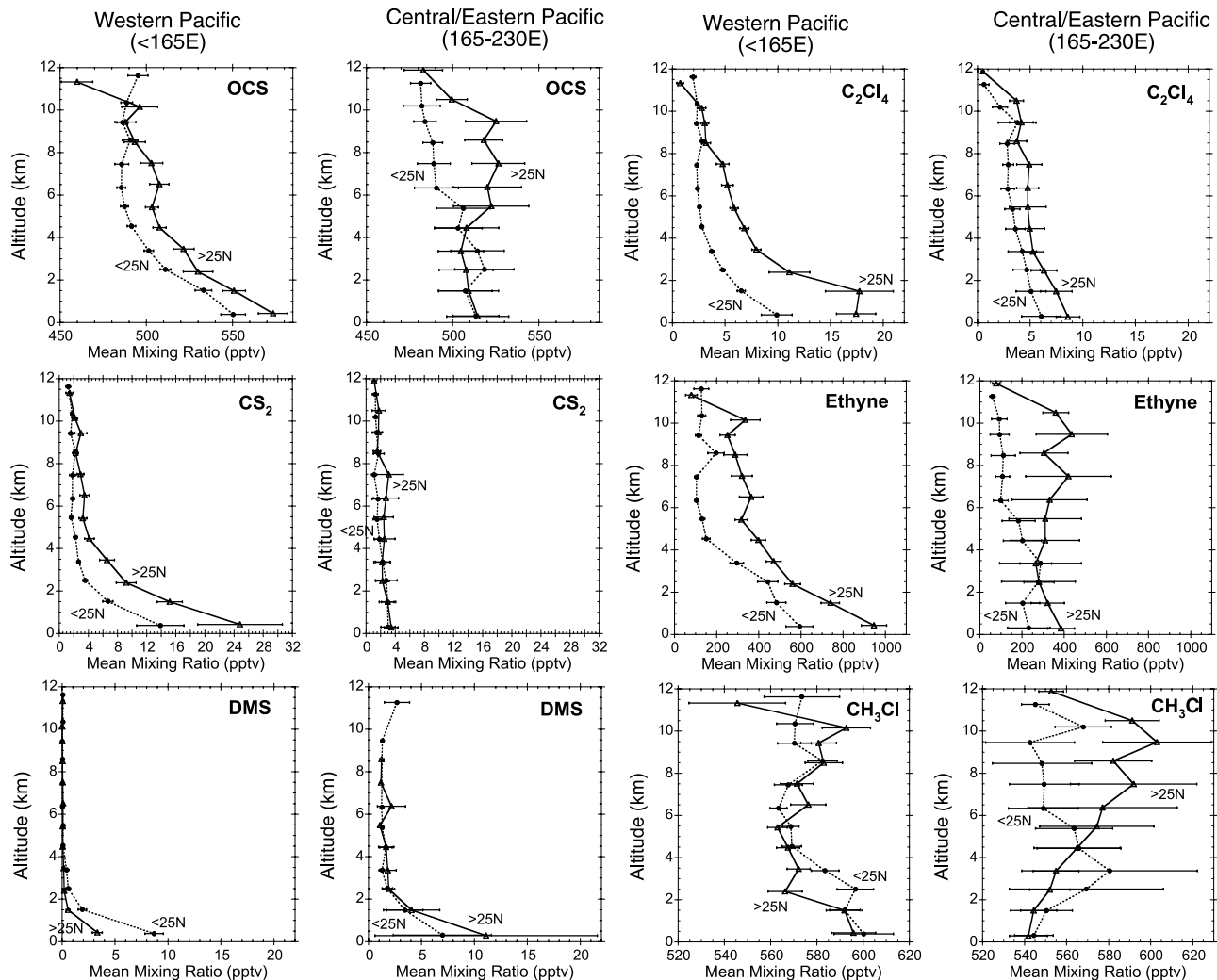
Figure 2

Figure 3. Mean vertical profiles for selected trace gases in 1 km altitude increments over the western Pacific (<165°E) and central/eastern Pacific (165°E−230°E) during TRACE-P. Error bars represent 95% confidence level of the mean.

good OCS versus CO correlations. Plumes with backward trajectories that intersected the vicinity of Beijing and Japan generally contained lower ratios of OCS and CS$_2$ versus CO$_2$ and CO, as well as lower CH$_3$Cl versus CO ratios, than the plumes that originated from the more southerly regions, Shanghai and Hong Kong, probably as the result of regional differences in fuel usage between biofuels and fossil fuel as well as biomass burning frequency [e.g., *Woo et al.*, 2003]. The one exception was that the ratio of OCS versus CO was slightly higher for the landing in Japan compared to Hong Kong. The particularly high ratios of OCS and CS$_2$ versus CO and CO$_2$ for the flight 13 Shanghai plume were accompanied by extremely high mixing ratios of SO$_2$ (up to 25 ppb). Because coal-fired power plants are the largest source for SO$_2$ in China [*Streets et al.*, 2003], this probably reflects locally heavy coal usage.

[26] As noted by *Blake et al.* [2003] and *Palmer et al.* [2003a], there appeared to be a strong local source of the

Montreal Protocol-regulated fire extinguisher gas Halon-1211 in the vicinity of Shanghai during TRACE-P. The Hong Kong and Japan plumes also show evidence of H-1211 emissions. The Beijing plumes are also well correlated for H-1211 versus CO but the ratios typically are an order of magnitude lower (Table 2).

5.2. "Pure" Biomass Burning Plumes

[27] The paucity of examples of "pure" biomass burning plumes that showed a significant correlation with CO or with CO$_2$ made it more difficult to investigate the contribution of biomass burning to the distributions of OCS and CS$_2$ during TRACE-P. We employed an air mass classification technique whereby we selected air masses that satisfied criteria for biomass burning (plus rural biofuel) influences (CH$_3$Cl > 625 pptv) but not urban influences (H-1211 < 4.35 pptv and C$_2$Cl$_4$ < 10 pptv). Note: because CH$_3$Cl is emitted from both biofuel and

Figure 2. Large-scale distributions of OCS and CS$_2$ as 2.5° × 2.5° latitude/longitude patches color-coded by average mixing ratio. The data are divided into three altitude ranges representing the lower troposphere (0−2 km), middle troposphere (2−8 km), and upper troposphere/lower stratosphere (8−12 km).
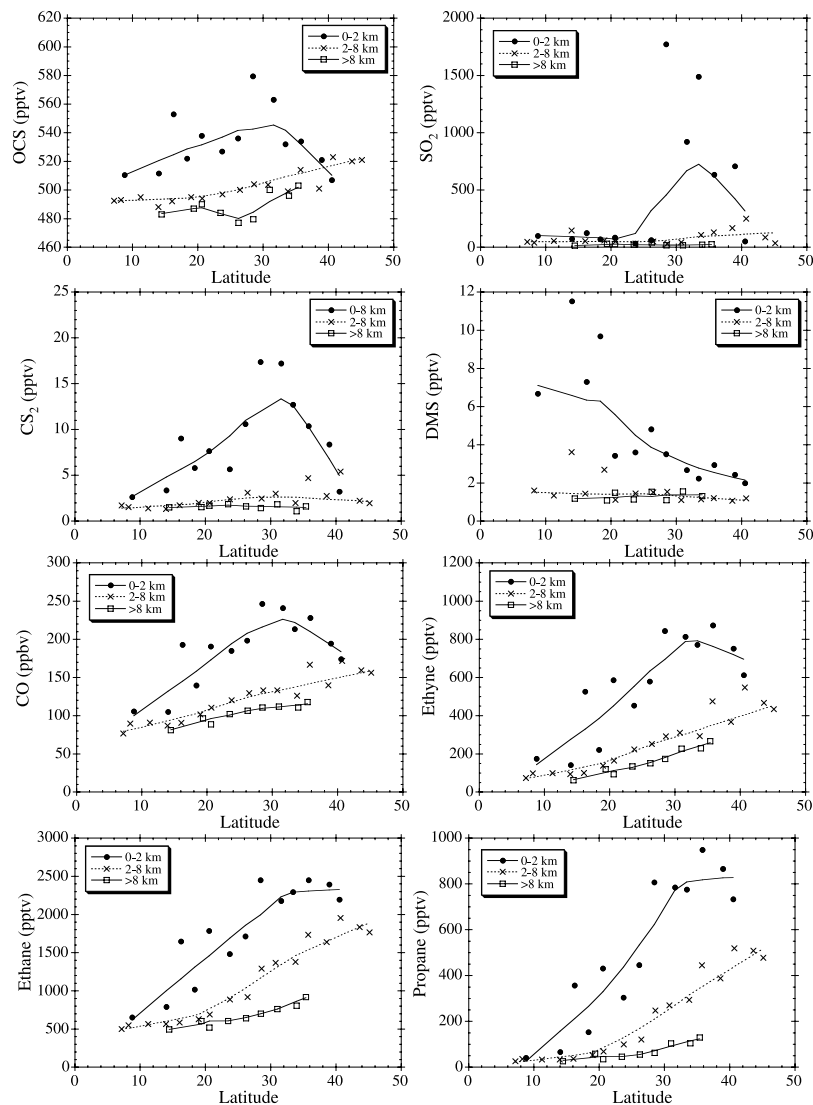
Figure 4. Mean latitude profiles for selected trace gases in 2.5° latitude increments over the western Pacific (<165°E) during TRACE-P. The data are divided into three altitude ranges: low (<2 km), middle (2–8 km), and (high > 8 km).

biomass burning sources this filter did not exclude biofuel emissions. For comparison, an "urban" subset of samples was defined as being sampled at low altitude (<2 km) over the western Pacific (west of 165°E) and containing

mixing ratios of the general urban tracer C$_2$Cl$_4$ greater than 10 pptv.

[28] Even though the correlation between OCS and CO was relatively poor for the biomass burning subset, the filter

Table 2. Emission Ratios for Selected Anthropogenic Plumes[a]

DC-8 Flight	Longitude, °E	Trajectory Path	n	ΔOCS/ΔCO Ratio × 10^{-3}	R^2	ΔCS$_2$/ΔCO Ratio × 10^{-3}	R^2	ΔOCS/ΔCO$_2$ Ratio × 10^{-6}	R^2	ΔCS$_2$/ΔCO$_2$ Ratio × 10^{-6}	R^2	ΔCH$_3$Cl/ΔCO Ratio × 10^{-3}	R^2	ΔH1211/ΔCO Ratio × 10^{-3}	R^2	ΔC$_2$Cl$_4$/ΔCO Ratio × 10^{-3}	R^2
8	128.67–132.35	north China-Beijing	17	0.35	0.62	0.07	0.34	7	0.87	1.7	0.66	NC		0.002	0.53	0.062	0.36
12	135.69–137.37	Beijing	14	0.61	0.91	0.23	0.73	9	0.51	5.3	0.97	0.40	0.85	0.003	0.95	0.083	0.77
13	124.79–125.99	north China-Beijing	8	0.72	0.93	0.20	0.94	26	0.85	7.2	0.84	0.30	0.94	0.001	0.86	0.051	0.96
12	121.07–122.11	China (Shanghai?)	7	0.94	0.99	0.42	0.87	30	0.99	15.3	0.99	2.06	0.96	0.011	0.98	0.041	0.99
13	125.04–125.11	Shanghai plume	21	0.96	0.95	0.96	0.69	46	0.84	48.8	0.68	1.21	0.85	0.020	0.75	0.103	0.82
13	131.2–139.09	landing in Japan	14	0.87	0.99	0.02	0.32	17	0.94	0.3	0.18	0.85	0.95	0.007	0.91	0.067	0.78
12	120.5–120.77	Hong Kong	10	0.78	0.92	0.48	0.72	22	0.95	15.6	0.98	1.63	0.87	0.011	0.88	0.065	0.94
Average				0.75		0.34		22		13.5		1.07		0.008		0.068	

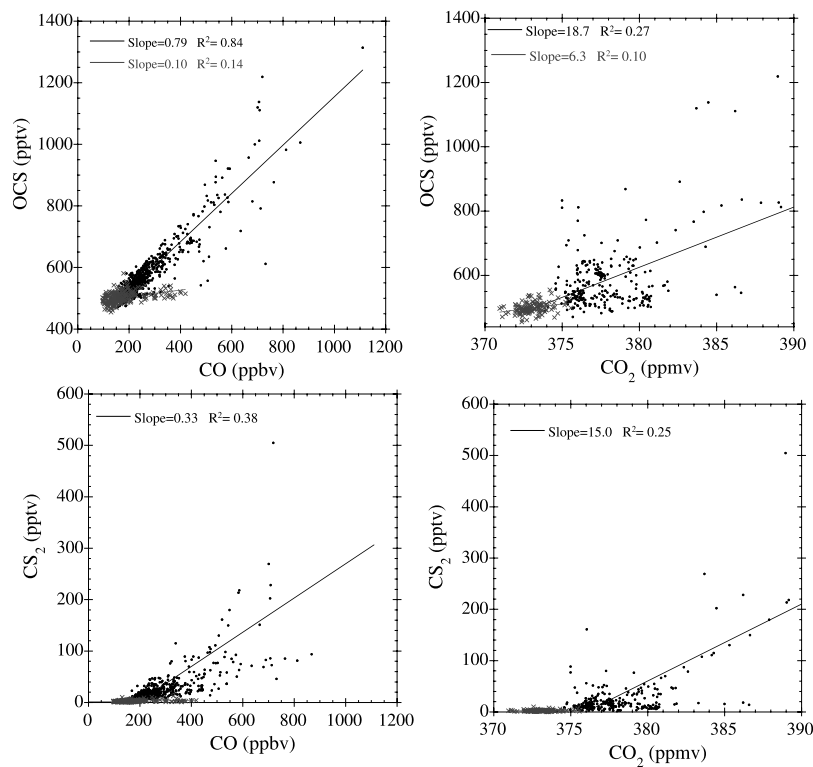[a]The n is number of samples; NC means not correlated.

Figure 5. Plots of OCS and CS$_2$ versus CO and CO$_2$ for two different air mass categories. The "urban mix" data (solid circles) were collected west of 165°E and at altitudes less than 2 km, with C$_2$Cl$_4$ mixing ratios greater than 10 pptv. "Pure biomass burning" data (grey crosses) are defined as all samples with CH$_3$Cl > 625 pptv, H-1211 < 4.35 pptv, and C$_2$Cl$_4$ < 10 pptv.

was successful in separating out two distinct data populations (Figure 5). The biomass burning samples revealed much lower enhancement ratios for OCS versus CO (approximately 0.1 pptv ppbv^{-1}) compared to the results for the urban data. This biomass burning ratio is roughly comparable to the value of 0.054 pptv ppbv^{-1} reported by *Meinardi et al.* [2003] for smoldering emissions from Australian brush fires.

[29] Enhancements of OCS versus CO$_2$ for the biomass burning data subset were also very low and poorly correlated and there was no significant correlation between CS$_2$ and CO or CO$_2$ for biomass burning. The relative lack of enhancements suggests that even though a great many of the urban plumes were mixed with biomass burning emissions [*Blake et al.*, 2003], the biomass burning component did not play a major role in determining the overall urban emission ratios for OCS or CS$_2$ during TRACE-P.

[30] The urban subset OCS/CO slope (0.79 pptv ppbv^{-1}) was very similar to the OCS/CO average for the individual urban plumes in Table 2 (0.75 pptv ppbv^{-1}). The urban OCS/CO$_2$ slope (Figure 5) was 18.7 pptv/ppmv ($R^2 = 0.27$), which is also a similar value to many of the urban plumes (average 22 pptv ppmv^{-1}) shown in Table 2.

6. Asian OCS and CS$_2$ Emissions

6.1. Air Mass Classification

[31] In order to make quantitative estimates of emissions from different regions of Asia we adopted a second air mass classification scheme based on the one devised by *Kita et al.*

[2002]. This scheme allowed us to link measured air mass signatures with the different regions/countries so that we could compare them to the emissions inventory data published by *Streets et al.* [2003].

[32] The paths of kinematic trajectories backward from the sampling points of the two NASA aircraft were examined. If a trajectory stayed below 800 hPa pressure level (for SE Asia case: below 450 hPa) for more than 6 hours in one of the four source regions (north China, south China, Japan + Korea, and continental SE Asia) shown in Figure 6, the air
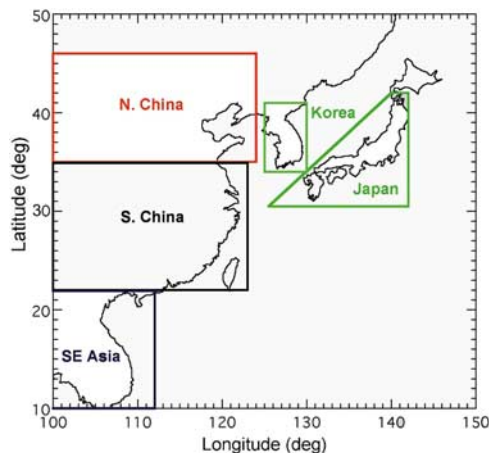

Figure 6. TRACE-P source region classifications. (Note that Korea and Japan were combined in this analysis.)
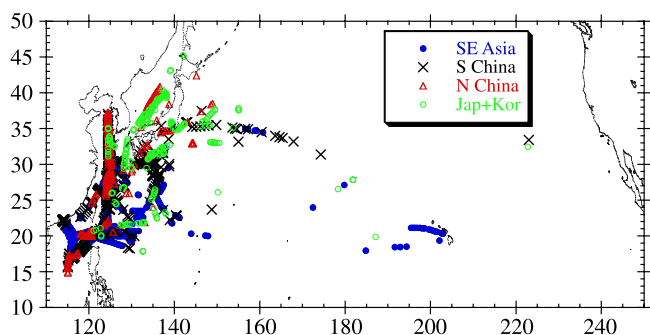
Figure 7. Location of DC-8 and P-3B TRACE-P samples categorized as in Figure 6.

mass was retained in our analysis and classified accordingly. If the trajectory stayed in two regions more than 6 hours, the air mass was excluded. The locations of the variously categorized samples are quite widespread across the latitude range sampled during TRACE-P (Figure 7). This explains why a simple latitudinal breakdown does not give a clear picture of regional emission trends.

6.2. Relationships With CO and CO$_2$

[33] Plots of the measured mixing ratios of OCS and CS$_2$ versus CO and CO$_2$ for air masses defined according to the classification scheme described above show that in general, both OCS and CS$_2$ correlate very well with CO and quite well with CO$_2$ (Figure 8). This suggests that during TRACE-P emissions of both OCS and CS$_2$ tend to be most closely linked with the same sources as CO (see also Table 2).

[34] Average OCS versus CO values for N and S China (Figure 8) are comparable to the values for individual urban plumes (Table 2), consistent with urban OCS and CS$_2$ emissions dominating these regions. However, the average slope for OCS versus CO for the Japan plus Korea category (Figure 8) was significantly higher than for the individual "landing in Japan" plume (Table 2). Conversely, the average values for CS$_2$ versus CO and CO$_2$ (Figure 8) were relatively high compared to the Japan plume (Table 2), indicating that urban Japanese emissions (or at least those for the Tokyo area where the TRACE-P planes landed) were not particularly representative of regional emissions. Indeed, the Tokyo air masses sampled appear to have contributed to the generally wider scatter for the Japan plus Korea plots compared to those for China (Figure 8).

[35] The OCS versus CO ratio for continental SE Asia of 0.18×10^{-3} is fairly similar to the value of 0.10 pptv ppbv^{-1} attributed earlier to "pure" biomass burning (continental SE Asia comprises Cambodia, Laos, Thailand and Vietnam). The OCS versus CO$_2$ value for continental SE Asia of 10.2×10^{-6} is also close to the mean $\Delta OCS/\Delta CO_2$ emission ratio of 11.4×10^{-6} reported by *Nguyen et al.* [1995] for biomass burning in east Asia. This strong
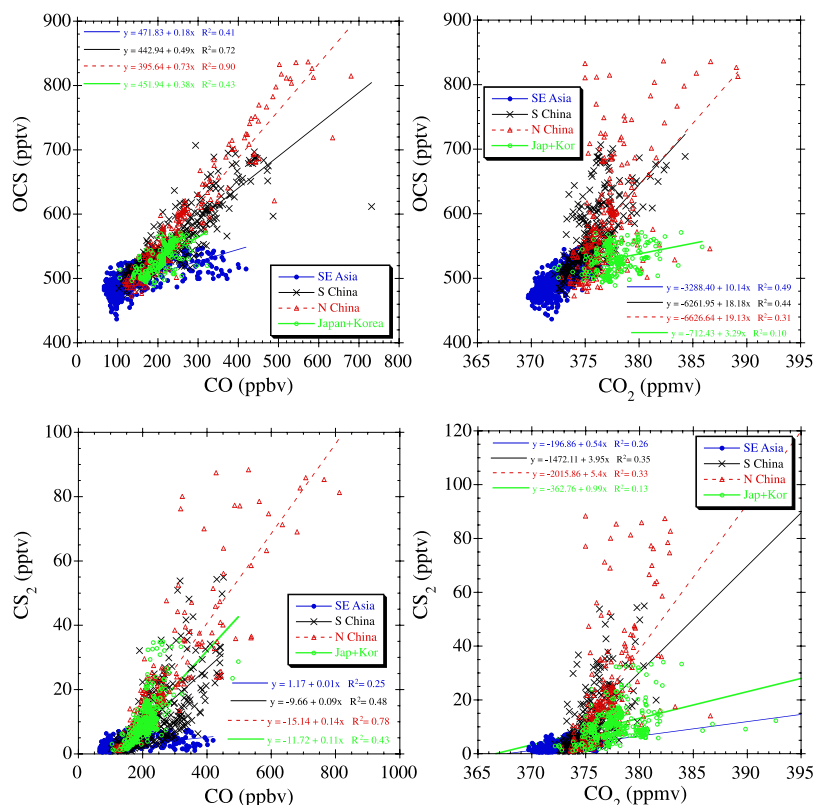

Figure 8. Plots of OCS and CS$_2$ versus CO and CO$_2$ for air masses defined in Figure 6. Continental SE Asia (blue solid circles), south China (black crosses), north China (red open triangles) and Japan plus Korea (green open circles). (Note that the highest 5% of the data have been removed to better represent regional averages.)

Table 3. Comparison of Annual Emissions of OCS and CS$_2$ Derived From Ratios With Those Derived From Our Anthropogenic Emissions Inventory[a]

	OCS Versus CO			OCS Versus CO$_2$			OCS Anthropogenic Inventory Emission, Gg	
	Ratio Versus CO, v/v × 10^{-3}	R^2	Calculated Emission From Slope, Gg	Ratio Versus CO$_2$, v/v × 10^{-6}	R^2	Calculated Emission From Slope, Gg		
North China	0.73 ± 0.03	0.90	51 (±3)	19 ± 5	0.31	30 (±8)		
South China	0.49 ± 0.03	0.72	52 (±4)	18 ± 2	0.44	41 (±5)		
China total			103 (±5)			71 (±9)	54	(±28)
Japan plus Korea	0.38 ± 0.06	0.43	10 (±2)	NC			14	(±7)
Continental SE Asia	0.18 ± 0.02	0.41	6.7 (± 0.7)	10 ± 1	0.49	5.9 (±0.5)	12	(±6)

	CS$_2$ Versus CO			CS$_2$ Versus CO$_2$			CS$_2$ Anthropogenic Inventory Emission, Gg	
	Ratio Versus CO, v/v × 10^{-3}	R^2	Calculated Emission From Slope, Gg	Ratio Versus CO$_2$, v/v × 10^{-6}	R^2	Calculated Emission From Slope, Gg		
North China	0.14 ± 0.01	0.78	18 (±2)	5.4 ± 1.0	0.33	15 (±2.8)		
South China	0.09 ± 0.01	0.48	18 (±3)	3.9 ± 0.6	0.35	16 (±2.5)		
China total			36 (±4)			32 (±3.8)	43	(±28)
Japan plus Korea	0.11 ± 0.02	0.43	6.3 (±0.8)	1.0 ± 0.3	0.13	3.0 (±0.9)	20	(±13)
Continental SE Asia	0.010 ± 0.002	0.25	0.7 (±0.1)	0.54 ± 0.08	0.26	0.56 (±0.08)	1.2	(±0.8)

[a]Continental SE Asia comprises emission estimates for Cambodia, Laos, Thailand, and Vietnam. China total includes emission estimates for Taiwan. NC means not correlated, and v/v is volume per volume.

biomass burning signature is consistent with biomass burning (together with biofuel emissions) being the most important OCS source in the continental SE Asian region (Figure 1 and Table 1).

6.3. Scaling to Emission Estimates

[36] The measured OCS and CS$_2$ versus CO and CO$_2$ ratios (Figure 8) were scaled up according to recent estimates of the regional emissions inventories for CO and CO$_2$ to produce the emissions estimates in Table 3. These regional values were taken directly from the work of *Streets et al.* [2003] who estimated 2000 Chinese emissions (including Taiwan) to be 118 Tg CO yr^{-1} and 4020 Tg CO$_2$ yr^{-1}.

6.4. Comparison of Results

[37] Calculated OCS emissions for China of 103 Gg yr^{-1} based on emission ratios were nearly double the 54 Gg yr^{-1} estimate using anthropogenic emission inventories (Table 3). The emissions estimate for China based on OCS versus CO$_2$ ratios was about 30% higher than the inventory estimate. By contrast, OCS emissions from Japan plus Korea based on CO ratios were quite similar to inventory values (taking into account the stated uncertainties), as were continental SE Asian values based on CO and CO$_2$.

[38] Chinese emission estimates for CS$_2$ derived by the two methods were very similar for CS$_2$ versus CO and CS$_2$ versus CO$_2$. The inventory values for continental SE Asia and Japan plus Korea were generally slightly higher than the calculated emission estimates.

6.5. Discussion of Comparison Results

[39] Some of the differences between the Chinese OCS inventory value and the observed ratios likely result from emissions from natural sources and to production of OCS from the oxidation of CS$_2$. Natural sources are very difficult to quantify, but are thought to be substantial on a global scale (Table 1). Oceans, soils and plants act as both sources and sinks of OCS [*Watts*, 2000]. Vegetation is thought to be

the main sink of atmospheric OCS [*Logan et al.*, 1979; *Brown and Bell*, 1986; *Toon et al.*, 1987; *Chin and Davis*, 1993]. Because TRACE-P was flown in the Asian spring, OCS soil and vegetation sinks are expected to be near seasonal lows [*Kettle et al.*, 2002b]. Soils may also be a net global sink of OCS [*Watts*, 2000].

[40] The oceans seasonally take up or out-gas OCS, with the winter-spring time being a period when open oceans on average act as a sink [*Watts*, 2000]. Therefore we expect the large-scale distribution of OCS to be dominated by sources associated with urban and industrial centers such as biofuel, coal and gasoline combustion, and industrial emissions. However, the global OCS and CS$_2$ budgets include significant components, about 15% and 10% of total sources, respectively [*Watts*, 2000]), from coastal oceanic emissions. As stated in 4.2 above, the similarity of the OCS and CS$_2$ vertical gradients close to the coast compared to DMS (Figure 3) indicates that a coastal oceanic source of these gases can not be ruled out. Although data are sparse, oceanic emissions of both OCS and CS$_2$ are associated with high levels of organic material, as in coastal areas and particularly estuaries [*Khalil and Rasmussen*, 1984; *Watts*, 2000; *Kettle et al.*, 2001]. As one of the largest rivers in the world, the Yangtze River exports tremendous amounts of organic carbon and other materials to the Asian continental shelf [*Degens et al.*, 1991]. The South China Sea is the largest ice-free marginal sea in the world and has significant runoff from several large rivers, including the Mekong and Pearl Rivers.

[41] To estimate upper limit coastal contributions (given that we expect emissions to be at a seasonal low for TRACE-P as already stated) we employed the average flux estimate for coastal oceans (including salt marshes and estuaries) of 0.20 ± 0.10 Tg yr^{-1} and 0.07 ± 0.04 Tg yr^{-1} for OCS and CS$_2$, respectively, from *Watts* [2000]. Scaling these values to total ocean shelf area (as compiled by *Watts* [2000]) gives emission values of approximately 40 and 14 t yr^{-1} per grid square for OCS and CS$_2$, respectively.

These emissions appear minor compared to combined terrestrial emissions of OCS and to northerly emissions of CS$_2$ (Figure 1), but not by comparison with northerly biomass burning emissions of OCS.

[42] To further estimate the impact of coastal emissions on our category basis we scaled average coastal emissions to ocean shelf areas for the individual countries (The Global Maritime Boundaries Database, EarthTrends, World Resources Institute, 2003, available at http://earthtrends.wri. org/text/COA/variables/62.htm). Employing this method, total Chinese coastal shelf emissions of OCS and CS$_2$ are estimated to be approximately 3.3 (±1.6) Gg yr^{-1} and 1.2 (±0.7) Gg yr^{-1}, respectively, which represent very minor contributions (less than 10% and within stated uncertainties) compared to the Chinese emissions estimates for both gases in Table 3. Coastal shelf emission estimates for Japan + Korea of approximately 2.3 (±1.2) Gg yr^{-1} and 0.8 (±0.4) Gg yr^{-1}, for OCS and CS$_2$, respectively, contribute a potentially higher proportion of total emissions compared to estimates in Table 3, but are still within the stated uncertainties for each estimate. The high values of OCS compared to CO for the "Landing in Japan" plume (Table 2) may also indicate localized coastal sources of OCS. For continental SE Asia, the lower overall emissions of OCS and CS$_2$ for this region mean that oceanic emissions of approximately 2.3 (±1.2) Gg yr^{-1} and 0.8 (±0.4) Gg yr^{-1}, respectively, may comprise up to 50% of OCS emissions and up to 100% of CS$_2$ emissions in Table 3. These values represent a small proportion of the global budget of these gases.

[43] The role played by CS$_2$ oxidation is also difficult to quantify. Globally, CS$_2$ oxidation has been estimated to account for ~30% of the atmospheric OCS source [*Chin and Davis*, 1993; *Watts*, 2000]. The lifetime of CS$_2$ is about 6 days (k_{OH} = 2 × 10^{-12} cm^3 molecule^{-1} s^{-1}) [*Chin and Davis*, 1993], which is long compared to the average transport time for industrial emissions from Japan and China to the TRACE-P sampling aircraft, especially from the many Chinese coastal cities [*Fuelberg et al.*, 2003]. This relatively fast transport would limit the amount of CS$_2$ conversion to OCS that would have taken place before sampling over the western Pacific. For example, we take the case of the Shanghai plume encountered during DC-8 flight 13 and determined by *Simpson et al.* [2003] to have a "photochemical age" of about 20 hours (2 in Shanghai + 18 during transit to the sampling aircraft). We assume an OCS yield from CS$_2$ oxidation of 0.83 ± 0.08 [*Stickel et al.*, 1993] and an average [OH] of 1 × 10^6 molecules cm^{-3}. The average CS$_2$ mixing ratio in the plume was 404 pptv, so we can calculate that the initial CS$_2$ mixing ratio (20 hours earlier) was about 466 pptv, giving a decay during transit of 62 pptv CS$_2$. This value equates to approximately 48 pptv (0.83 × 62 pptv) of OCS being produced in the plume between emission and sampling. The average plume mixing ratio of OCS was 1079 pptv and a representative background OCS value was 515 pptv. Therefore the component of OCS contributed by CS$_2$ oxidation represented only about 8% of the excess OCS above background contained in the plume at sampling. Natural coastal CS$_2$ emissions would contribute a similarly small proportion of what have already estimated to be relatively small emissions to coastal Asian levels of OCS. Obviously, the CS$_2$ would contribute

progressively more OCS (up to 83% of total CS$_2$ emissions [*Stickel et al.*, 1993]) as the air masses age further.

[44] The lower Chinese OCS source estimate obtained by the inventory may also reflect the scarcity of data characterizing important Chinese OCS source categories. Much of Chinese fossil fuel usage in the domestic sector is dominated by coal and, as in most of developing Asia, equipment performance is poor and CO emissions are high. CO emission factors for Asian small coal combustors are 2–3 times higher than comparable sources in the west [*USEPA*, 2003]. By contrast, American coal-fired power plants use more sophisticated (and expensive) pollution abatement technologies to control coal-burning emissions [*Tomeczek et al.*, 2000]. Our observation that OCS and CO are very well correlated (Figure 8) leads us to speculate that OCS emissions, like CO emissions, are likely to be highly dependent on the efficiency of the combustion process and the operation and maintenance of combustion equipment. *Woo et al.* [2003] reported a distinct gradient in regional CO versus CO$_2$ ratios for China that was related to significant differences between regional fuel usage. Therefore emission ratios for OCS versus CO$_2$ also are likely to be sensitive to combustion conditions and fuel type/quality. There has been a recent decline in coal usage and an improvement in the quality of coal burned within China, but there still may be regions in central China where the use of cheap, poor quality (and high sulfur) coal continues [*Streets et al.*, 2003]. However, as stated earlier, we were forced to use the only available measured OCS versus CO emission ratio for coal burning, which corresponds to a coal-fired Power Plant in Denver, CO, to represent all coal combustors in Asia for the inventory. Only a single Chinese measurement for a coal stove in Beijing was available to support this value.

[45] A further, rather speculative possibility is that coal mine fires make a significant contribution to Chinese sulfur gas emissions. Coal mine fires have been touted as a major environmental catastrophe in China, however, Chinese and other western authorities believe that the amount of coal consumed in out of control burning is probably only about 14 × 10^6 t annually, yielding 490 Gg CO or 0.4% of China's total CO emissions [*Streets et al.*, 2003]. Even so, the smoldering combustion associated with these fires could emit large amounts of reduced sulfur gases, including OCS.

[46] In any case, it is clear that many more measurements of OCS emission ratios are needed to properly characterize Chinese sources of this gas.

[47] *Carmichael et al.* [2003] recently suggested that there is a problem with the CO inventory for China, probably associated with the relative importance of biofuel and fossil fuel in the domestic sector emission estimates for central China. An inverse modeling study by *Palmer et al.* [2003b] also indicated that the 2000 Chinese CO emissions inventory values are underestimated and should be increased by 30%. Increasing Chinese CO emission estimates for this work would make the agreement between our measured ratio-based OCS emission estimates with inventory OCS values worse. In addition, the good correlation between OCS and CO that we observed indicates that increased CO emissions would be accompanied by proportionally higher OCS emissions (i.e., if we add extra sources to the CO inventory we should also correspondingly in-

crease OCS inventory emissions). Therefore changing CO emissions alone would likely not be appropriate in this case.

7. Conclusions

[48] We present a new inventory of anthropogenic Asian emissions (including biomass burning) for OCS and CS$_2$. This inventory assumes natural emissions were near zero during the spring TRACE-P time period. Results from TRACE-P measurements confirm that OCS and CS$_2$ mixing ratios over the western Pacific basin were influenced strongly by land-based, anthropogenic sources during TRACE-P. Some of the highest mixing ratios of OCS (e.g., 850 pptv) and CS$_2$ (e.g., 90 pptv) were observed in plumes of polluted air transported from the northern part of China (north of 35°N). These plumes also showed a strong correlation ($R^2 = 0.90$) with CO and other anthropogenic pollution markers.

[49] Distinctly different ratios of OCS versus CO were associated with urban-type air masses and with those characterized as biomass burning air masses. The strong association of continental SE Asia emissions with OCS versus CO relationships characteristic of biomass burning/biofuel suggests that SE Asian OCS levels are dominated by biomass burning/biofuel emissions.

[50] Comparison between emissions of OCS and CS$_2$ based on their observed ratios with CO and CO$_2$ and our emission inventory estimates for four different Asian regions revealed generally good agreement, especially for CS$_2$. However, the inventory estimates for Chinese OCS emissions appear low, possibly due to natural sources (which were neglected because they were predicted to play a minor role in spring), or more likely because emission ratios from certain urban/industrial emissions such as coal burning are not well characterized for China.

References

Andreae, M. O., and P. J. Crutzen (1997), Atmospheric aerosols: Biogeochemical sources and role in atmospheric chemistry, *Science*, *276*, 1052–1056.

Andreae, M. O., and P. Merlet (2001), Emissions of trace gases and aerosols from biomass burning, *Global Biogeochem. Cycles*, *15*, 955–966.

Aydin, M., W. J. De Bruyn, and E. S. Saltzman (2002), Preindustrial atmospheric carbonyl sulfide (OCS) from an Antarctic ice core, *Geophys. Res. Lett.*, *29*(9), 1359, doi:10.1029/2002GL014796.

Banwart, W. L., and J. M. Bremner (1975), Identification of sulfur gases evolved from animal manures, *J. Environ. Qual.*, *4*, 363–366.

Bandy, A. R., D. C. Thornton, and J. E. Johnson (1993), Carbon disulfide measurements in the atmosphere of the western North Atlantic and the northwestern South Atlantic Oceans, *J. Geophys. Res.*, *98*, 23,449–23,457.

Blake, N. J., D. R. Blake, B. C. Sive, T.-Y. Chen, J. E. Collins Jr., G. W. Sachse, B. E. Anderson, and F. S. Rowland (1996), Biomass burning emissions and vertical distribution of atmospheric methyl halides and other reduced carbon gases in the South Atlantic region, *J. Geophys. Res.*, *101*, 24,151–24,164.

Blake, N. J., et al. (1999), Influence of Southern Hemispheric biomass burning on mid-tropospheric distributions of nonmethane hydrocarbons and selected halocarbons over the remote South Pacific, *J. Geophys. Res.*, *104*, 16,213–16,232.

Blake, N., et al. (2003), NMHCs and halocarbons in Asian continental outflow during the Transport and Chemical Evolution over the Pacific (TRACE-P) field campaign: Comparison with PEM-West B, *J. Geophys. Res.*, *108*(D20), 8806, doi:10.1029/2002JD003367.

Brown, K. A., and J. N. B. Bell (1986), Vegetation: The missing link in the global cycle of OCS, *Atmos. Environ.*, *20*, 537–540.

Carmichael, G. R., et al. (2003), Regional-scale chemical transport modeling in support of the analysis of observations obtained during the TRACE-P experiment, *J. Geophys. Res.*, *108*(D21), 8823, doi:10.1029/2002JD003117.

Charlson, R. J., J. Langner, and H. Rodhe (1990), Sulphate aerosol and climate, *Nature*, *348*, 22.

Chin, M., and D. D. Davis (1993), Global sources and sinks of carbonyl sulfide and carbon disulfide and their distributions, *Global Biogeochem. Cycles*, *7*, 321–337.

China National Chemical Information Centre (2000), *China Chemical Industry Yearbook 2000*, Beijing.

Colman, J. J., A. L. Swanson, S. Meinardi, B. C. Sive, D. R. Blake, and F. S. Rowland (2001), Description of the analysis of a wide range of volatile organic compounds in whole air samples collected during PEM-Tropics A and B, *Anal. Chem.*, *73*, 3723–3731.

Crutzen, P. J. (1976), The possible importance of OCS for the sulfate layer of the stratosphere, *Geophys. Res. Lett.*, *3*, 73–76.

Degens, E. T., , S. Kempe, and J. E. Richey (Eds.) (1991), *Biogeochemistry of Major World Rivers*, *SCOPE Rep. 42*, John Wiley, Hoboken, N. J. (available at www.icsu-scope.org/downloadpubs/scope42/)

Fried, A., B. Henry, R. A. Ragazzi, M. Merrick, J. Stokes, T. Pyzdrowski, and R. Sams (1992), Measurements of carbonyl sulfide in automotive emissions and an assessment of its importance to the global sulfur cycle, *J. Geophys. Res.*, *97*, 14,621–14,634.

Fuelberg, H. E., C. M. Kiley, J. R. Hannan, D. J. Westberg, M. A. Avery, and R. E. Newell (2003), Meteorological conditions and transport pathways during the Transport and Chemical Evolution over the Pacific (TRACE-P) experiment, *J. Geophys. Res.*, *108*(D20), 8782, doi:10.1029/2002JD003092.

Harnisch, J., R. Borchers, P. Fabian, and K. Kourtidis (1995), Aluminum production as a source of atmospheric carbonyl sulfide (COS), *Environ. Sci. Pollut. Res.*, *2*, 161–162.

Heald, C. L., D. J. Jacob, P. I. Palmer, M. J. Evans, G. W. Sachse, H. B. Singh, and D. R. Blake (2003), Biomass burning emission inventory with daily resolution: Application to aircraft observations of Asian outflow, *J. Geophys. Res.*, *108*(D21), 8811, doi:10.1029/2002JD003082.

Jacob, D. J., J. Crawford, M. M. Kleb, V. S. Connors, R. J. Bendura, J. L. Raper, G. W. Sachse, J. Gille, L. Emmons, and J. C. Heald (2003), Transport and chemical evolution over the Pacific (TRACE-P) mission: Design, execution, and first results, *J. Geophys. Res.*, *108*(D20), 9000, doi:10.1029/2002JD003276.

Kanda, K., H. Tsuruta, and K. Minami (1992), Emissions of DMS, OCS and CS$_2$ from paddy fields, *Jpn. J. Soil Sci. Plant Nutrition*, *38*, 709–716.

Kettle, A. J., T. S. Rhee, M. von Hobe, A. Poulton, J. Aiken, and M. O. Andreae (2001), Assessing the flux of different volatile sulfur gases from the ocean to the atmosphere, *J. Geophys. Res.*, *106*, 12,193–12,209.

Kettle, A. J., U. Kuhn, M. von Hobe, J. Kesselmeier, and M. O. Andreae (2002a), Global budget of atmospheric carbonyl sulfide: Temporal and spatial variations of the dominant sources and sinks, *J. Geophys. Res.*, *107*(D22), 4658, doi:10.1029/2002JD002187.

Kettle, A. J., U. Kuhn, M. von Hobe, J. Kesselmeier, and M. O. Andreae (2002b), Comparing forward and inverse models to estimate the seasonal variation of hemisphere-integrated fluxes of carbonyl sulfide, *Atmo. Chem. Phys.*, *2*, 343–361.

Khalil, M. A. K., and R. A. Rasmussen (1984), Global sources, lifetimes and mass balances of carbonyl sulfide (OCS) and carbon disulfide (CS$_2$) in the Earth's atmosphere, *Atmos. Environ.*, *18*, 1805–1813.

Kita, K., et al. (2002), Sources, distribution and partitioning of reactive nitrogen in the lower troposphere over western Pacific during TRACE-P, *Eos Trans. AGU*, *83*(47), Fall Meet. Suppl., Abstract A62A-0134.

Liu, H., D. J. Jacob, I. Bey, R. Yantosca, B. N. Duncan, and G. W. Sachse (2003), Transport pathways for Asian pollution outflow over the Pacific: Interannual and seasonal variations, *J. Geophys. Res.*, *108*(D20), 8786, doi:10.1029/2002JD003102.

Logan, J. A., M. B. McElroy, and M. J. Prather (1979), Oxidation of CS$_2$ and OCS: SO sources for atmospheric SO$_2$, *Nature*, *281*, 185–188.

Meinardi, S., I. J. Simpson, N. J. Blake, D. R. Blake, and F. S. Rowland (2003), Dimethyl disulfide (DMDS) and dimethyl sulfide (DMS) emissions from biomass burning in Australia, *Geophys. Res. Lett.*, *30*(9), 1454, doi:10.1029/2003GL016967.

Mu, Y., H. Wu, X. Zhang, and G. Jiang (2002), Impact of anthropogenic sources on carbonyl sulfide in Beijing City, *J. Geophys. Res.*, *107*(D24), 4769, doi:10.1029/2002JD002245.

Nguyen, B. C., N. Mihalopoulos, J. P. Putaud, and B. Bonsang (1995), Carbonyl sulfide emissions from biomass burning in the tropics, *J. Atmos. Chem.*, *22*(1/2), 55–65.

Notholt, J., et al. (2003), Enhanced upper tropical tropospheric COS: Impact on the stratospheric aerosol layer, *Science*, *300*, 307–310.

Palmer, P. I., D. J. Jacob, L. J. Mickley, D. R. Blake, G. W. Sachse, H. E. Fuelberg, and C. M. Kiley (2003a), Eastern Asian emissions of anthropogenic halocarbons deduced from aircraft concentration data, *J. Geophys. Res.*, *108*(D24), 4753, doi:10.1029/2003JD003591.

Palmer, P. I., D. J. Jacob, D. B. A. Jones, C. L. Heald, R. M. Yantosca, J. A. Logan, G. W. Sachse, and D. G. Streets (2003b), Inverting for emissions of carbon monoxide from Asia using aircraft observations over the western Pacific, *J. Geophys. Res.*, *108*(D21), 8828, doi:10.1029/2003JD003397.

Peyton, T. O., R. V. Steele, and W. R. Mabey (1976), Carbon disulfide, carbonyl sulfide: Literature review and environmental assessment, *Rep. EPA-600/9-78-009*, U.S. Environ. Protect. Agency, Washington, D. C.

Sachse, G. W., G. F. Hill, L. O. Wade, and M. G. Perry (1987), Fast-response, high-precision carbon monoxide sensor using a tunable diode laser absorption technique, *J. Geophys. Res.*, *92*, 2071–2081.

Simpson, I. J., N. J. Blake, D. R. Blake, E. Atlas, F. Flocke, J. H. Crawford, H. E. Fuelberg, C. M. Kiley, S. Meinardi, and F. S. Rowland (2003), Photochemical production and evolution of selected C$_2$–C$_5$ alkyl nitrates in tropospheric air influenced by Asian outflow, *J. Geophys. Res.*, *108*(D20), 8808, doi:10.1029/2002JD002830.

Streets, D., et al. (2003), An inventory of gaseous and primary aerosol emissions in Asia in the year 2000, *J. Geophys. Res.*, *108*(D21), 8809, doi:10.1029/2002JD003093.

Stickel, R. E., M. Chin, E. P. Daykin, A. J. Hynes, P. H. Wine, and T. J. Wallington (1993), Mechanistic studies of the OH-initiated oxidation of CS$_2$ in the presence of O$_2$, *J. Phys. Chem.*, *97*(51), 13,653–13,661.

Tomeczek, J., J. Goral, J. Ochman, L. Dobrowolski, Katedra Energetyki Procesowej, and Politechnika Slaska, Katowice, Poland (2000), Low-emission EPK gas burners for modernization of boilers for heating systems, *Gospodarka Paliwami Energia*, *48*(5), 15–19.

Toon, O. B., J. B. Kasting, R. P. Turco, and M. S. Liu (1987), The sulfur cycle in the marine atmosphere, *J. Geophys. Res.*, *92*, 943–963.

Turco, R. P., R. C. Whitten, O. B. Toon, J. B. Pollack, and P. Hamill (1980), OCS, stratospheric aerosols and climate, *Nature*, *283*, 283–286.

United Nations (UN) (1998), Industrial commodity statistics yearbook 1996, *Rep. ST/ESA/STAT/SER. P/36*, Dep. of Econ. and Social Affairs, New York.

U.S. Environmental Protection Agency (USEPA) (1992), Global methane emissions from livestock and poultry manure, *Rep. EPA/400/1-91/048*, Washington, D. C.

U.S. Environmental Protection Agency (USEPA) (2003), *Compilation of Air Pollutant Emission Factors,* vol. I, *Stationary Point and Area Sources*, AP-42, 5th ed., Washington, D. C.

Vay, S. A., B. E. Anderson, T. J. Conway, G. W. Sachse, J. E. Collins Jr., D. R. Blake, and D. J. Westberg (1999), Airborne observations of the tropospheric CO$_2$ distribution and its controlling factors over the South Pacific Basin, *J. Geophys. Res.*, *104*(D5), 5663–5676.

Watts, S. F. (2000), The mass budgets of carbonyl sulfide, dimethyl sulfide, carbon disulfide and hydrogen sulfide, *Atmos. Environ.*, *34*, 761–779.

Woo, J.-H., et al. (2003), Contribution of biomass and biofuel emissions to trace gas distributions in Asia during the TRACE-P experiment, *J. Geophys. Res.*, *108*(D21), 8812, doi:10.1029/2002JD003200.

Xu, X., H. G. Bingemer, and U. Schmidt (2002), An empirical model for estimating the concentration of carbonyl sulfide in surface seawater from satellite measurements, *Geophys. Res. Lett.*, *29*(9), 1316, doi:10.1029/2001GL014252.

————————————

E. Atlas, National Center for Atmospheric Research, 1850 Table Mesa Drive, Boulder, CO 80307, USA. (atlas@ucar.edu)

M. A. Avery, G. Sachse, and S. A. Vay, NASA Langley Research Center, Mail Stop 472, Hampton, VA 23681-0001, USA. (m.a.avery@larc.nasa.gov; g.w.sachse@larc.nasa.gov; s.a.vay@larc.nasa.gov)

D. R. Blake, N. J. Blake, S. Meinardi, F. S. Rowland, and I. J. Simpson, Department of Chemistry, University of California, 516 Rowland Hall, Irvine, CA 92697-2025, USA. (drblake@uci.edu; nblake@uci.edu; smeinard@uci.edu; rowland@uci.edu; isimpson@uci.edu)

A. R. Bandy and D. C. Thornton, Chemistry Department, Drexel University, 32nd and Chestnut Streets, Philadelphia, PA 19104, USA. (bandyar@drexel.edu; dct@drexel.edu)

J. E. Dibb and R. W. Talbot, EOS, CCRC, Morse Hall, University of New Hampshire, Durham, NH 03824, USA. (jack.dibb@unh.edu; robert.talbot@unh.edu)

H. E. Fuelberg, Department of Meteorology, Florida State University, 404 Love Building, Tallahassee, FL 32306, USA. (fuelberg@huey.met.fsu.edu)

J. Green, Division of Chemistry and Chemical Engineering, M/C 127-72, California Institute of Technology, Pasadena, CA 91125, USA. (jegreen@caltech.edu)

K. Kita, Department of Environmental Sciences, Faculty of Science, Ibaraki University, 2-1-1 Bunkyo, Mito, Ibaraki 310-8512, Japan. (kita@mx.ibaraki.ac.jp)

D. G. Streets, Argonne National Laboratory, 9700 South Cass Avenue, Argonne, IL 60439, USA. (dstreets@anl.gov)

J.-H. Woo, Center for Global and Regional Environmental Research, 252 Iowa Advanced Technology Labs, University of Iowa, Iowa City, IA 52242, USA. (woojh21@cgrer.uiowa.edu)